Science Translational Medicine AAAS

Bioengineering Dermo-Epidermal Skin Grafts with Blood and Lymphatic Capillaries

Daniela Marino *et al.*

Sci Transl Med **6**, 221ra14 (2014);
DOI: 10.1126/scitranslmed.3006894

Editor's Summary

Skin Grafts Need Plumbing, Too

To help heal a severe burn or wound, clinicians surgically transplant skin grafts, which consist of the epidermis (outer skin layer) and, often, part of the dermis (deeper layer, directly below the epidermis). The success of these grafts, however, is limited by the ability of blood vessels to form in the newly transplanted skin and deliver nutrients to the cells. Research has also suggested that the lymphatics may be necessary for skin graft survival, by essentially d raining immune cells, debris, and excess fluid from the wounded area. Here, Marino, Luginbühl, and colleagues engineered a skin graft that wasn't just the patient's skin cells—it also contained both lymph and blood capillaries "prevascularized" ex vivo and then transplanted onto a wound.

The authors created the dermo-epidermal skin grafts by taking cells from human foreskin, called human dermal microvascular endothelial cells (HDMECs), and embedding them in three-dimensional hydrogels. HDMECs consist of a mixture of both lymphatic endothelial cells and blood vessel endothelial cells, so both types of functional capillaries —blood and lymph—formed from these cells in vitro in the fibrin or collagen hydrogels. Moving in vivo, the authors transplanted engineered skin grafts containing the HDMECs as well as human fibroblasts and keratinocyes—two cell types found in skin—onto the wounded backs of nude rats (animals without an immune system). Marino, Luginbühl, *et al* . reported that the human skin grafts formed the expected skin layers after 2 weeks, connected with existing rat lymphatic capillaries, and drained fluid away from the wound.

Although testing and characterization are still needed in animals with an immune system and with skin similar to humans (such as a pig), these engineered dermo-epidermal hydrogels potentially represent the next generation of skin grafts, complete with the vascular and lymphatic plumbing and ready to transplant.

Science Translational Medicine (print ISSN 1946-6234; online ISSN 1946-6242) is published weekly, except the last week in December, by the American Association for the Advancement of Science, 1200 New York Avenue NW, Washington, DC 20005.

BIOENGINEERING

Bioengineering Dermo-Epidermal Skin Grafts with Blood and Lymphatic Capillaries

Daniela Marino,[1]* Joachim Luginbühl,[1]* Simonetta Scola,[1] Martin Meuli,[2] Ernst Reichmann[1]†

The first bioengineered, autologous, dermo-epidermal skin grafts are presently undergoing clinical trials; hence, it is reasonable to envisage the next clinical step at the forefront of plastic and burn surgery, which is the generation of autologous skin grafts that contain vascular plexuses, preformed in vitro. As the importance of the blood, and particularly the lymphatic vascular system, is increasingly recognized, it is attractive to engineer both human blood and lymphatic vessels in one tissue or organ graft. We show here that functional lymphatic capillaries can be generated using three-dimensional hydrogels. Like normal lymphatics, these capillaries branch, form lumen, and take up fluid in vitro and in vivo after transplantation onto immunocompromised rodents. Formation of lymphatic capillaries could be modulated by both lymphangiogenic and anti-lymphangiogenic stimuli, demonstrating the potential usefulness of this system for in vitro testing. Blood and lymphatic endothelial cells never intermixed during vessel development, nor did blood and lymphatic capillaries anastomose under the described circumstances. After transplantation of the engineered grafts, the human lymphatic capillaries anastomosed to the nude rat's lymphatic plexus and supported fluid drainage. Successful preclinical results suggest that these skin grafts could be applied on patients suffering from severe skin defects.

INTRODUCTION

The critical importance of the lymphatic system in the human body becomes increasingly evident. Consequently, the tissue engineering of lymphatic organs (lymphatic vessels, lymph nodes, spleens, and cells derived from lymphatic organs) not only generates valuable ex vivo research models but also allows the transplantation of these organs to repair or improve lymphatic deficiencies caused by disease or injury (*1*).

Our research focuses on the bioengineering of full-thickness skin analogs: dermo-epidermal skin substitutes with physiological, structural, and functional properties (*2*). A central issue of this approach is the in vitro generation of a preexisting network of capillaries (*3*), which significantly supports perfusion of the dermal component, hence, providing rapid and efficient access to oxygen and nutrients, which assures rapid take, proliferation, and differentiation of the skin transplant (*2*). Prevascularized dermo-epidermal skin substitutes were generated using primary human endothelial cells and sophisticated biological matrices (*4*–*7*). So far, however, limited data are available on the bioengineering of functional human lymphatic capillaries or on the integration of a dermal lymphatic network in skin grafts.

In the human dermis, lymphatic vessels play a major role in tissue fluid homeostasis and immune cell trafficking (*8*). Dermal lymphatic capillaries exhibit a wide lumen, anchoring filaments, and no or an incomplete basement membrane, and lack mural cell coverage. These features enable lymphatic capillaries to respond to interstitial liquid pressure by taking up and removing excess tissue fluid (*8*, *9*). After wounding, also the lymphatic endothelium is ruptured; thus, the draining capacity of the lymphatic vessels is compromised. As a consequence, accumulation of tissue fluid, that is, lymphedema, seroma, or lymphoceles (*10*–*12*), arises. Persistent local interstitial fluid, as well as delayed removal of local debris and inflammatory cells, impedes wound healing. In contrast, induction of lymphangiogenesis and immune cell recruitment were shown to accelerate skin regeneration (*13*). Therefore, to achieve a physiologically relevant dermal tissue complexity, and accelerate skin tissue regeneration after graft transplantation, a skin graft containing both blood and lymphatic vessels would ideally serve to efficiently reconstitute a full-thickness skin defect.

This study demonstrates the in vitro bioengineering and in vivo grafting of a human dermo-epidermal skin substitute prevascularized by both lymphatic and blood capillaries. Both the pure population of human lymphatic endothelial cells (hLECs; isolated from human foreskin) and the hLEC fraction present in human dermal microvascular endothelial cells (HDMECs; isolated from human foreskin) developed into lumen-forming bona fide lymphatic capillaries in vitro within 21 days in either fibrin or collagen type I hydrogels. We confirmed the lymphatic nature of the engineered microvessels by showing that they presented anchoring filaments, expressed all major lymphatic markers, and could be modulated by both lymphangiogenic and anti-lymphangiogenic stimuli.

Lymphatic functionality was confirmed by demonstrating that the bioengineered lymphatic microvessels took up fluid from the interstitial space in vitro and triggered fluid drainage in vivo. Grafting studies in vivo revealed that the engineered lymphatic microvessels maintained their lumens as well as their typical characteristics, such as the absence of a complete basement membrane and the lack of mural cell coverage. We found that bioengineered human lymphatics anastomosed to the recipient's lymphatics as early as 14 days after transplantation. When transplanted onto immunoincompetent rats, the prevascularized dermis supported the development of the epidermis, indicating that it may, in the future, be possible to translate these prevascularized dermo-epidermal substitutes into clinical application.

RESULTS

Bioengineering of human lumen-forming lymphatic capillaries in three-dimensional hydrogels in vitro

The identification of markers specific for the lymphatic vascular lineage has made it possible to isolate hLECs at high purity from human dermis

[1]Tissue Biology Research Unit, Department of Surgery, University Children's Hospital Zurich, August Forel-Strasse 7, 8008 Zurich, Switzerland. [2]Department of Surgery, University Children's Hospital, Steinwiesstrasse 75, 8032 Zurich, Switzerland.
*These authors contributed equally to this work.
†Corresponding author. Email: ernst.reichmann@kispi.uzh.ch

by either fluorescence-activated cell sorting (FACS) or magnetic-activated cell sorting (*14*). Prox1, a marker of human lymphatic vessels (*15*, *16*), was homogeneously expressed by hLECs in conventional cell culture (Fig. 1A). Confluent hLEC monolayers assembled into cord-like structures when overlaid with collagen type I gels for up to 20 hours in vitro (Fig. 1B). These cords, often referred to as tube-like structures in a tube formation assay, are somehow reminiscent of the morphology of microvessels. However, under these in vitro circumstances, lumen formation did not occur (Fig. 1B).

Using a method that we had established previously for HDMECs (*7*), we investigated whether hLECs would similarly arrange into lumen-forming true capillaries in both fibrin and type I collagen hydrogel; indeed, hLECs developed into branching capillaries (Fig. 1, C, D, and F), as revealed by staining for CD31—a pan-endothelial cell marker—3 weeks after coculture with 40% human dermal fibroblasts. Notably, capillary formation did not occur in the absence of fibroblasts (Fig. 1, E and F). Likewise, neither fibroblast-conditioned medium, the addition of vascular endothelial growth factor–A (VEGF-A) or VEGF-C, nor the presence of fibroblasts on the underside of a Transwell system induced capillary formation in hLECs (Fig. 1F). Hence, the physical contact between human dermal fibroblasts and LECs was a requisite for the development of true branching lymphatic capillaries in the hydrogel. Histology revealed that the engineered capillaries developed a continuous lumen of physiological size (17 to 60 μm) (Fig. 1G), with an average lumen diameter of 28 + 10.67 μm (+SEM, 25 lymphatic vessels analyzed per five hydrogels) measured on whole-mount specimens.

The lymphatic nature of the capillaries was confirmed by double immunofluorescence staining performed on whole-mount hydrogel preparations. The bioengineered lymphatic capillaries expressed CD31 (Fig. 2A) and the lymphatic-specific nuclear transcription factor Prox1 (Fig. 2, A to D). Most of the capillaries showed a physiological size (10 μm in diameter) (*17*) of the nuclei (Fig. 2B). Two other lymphatic vascular markers, Lyve-1 (Fig. 2C) and podoplanin (Fig. 2D), confirmed the lymphatic nature of the bioengineered human capillaries.

Modulation of capillary formation by pro- and anti-lymphangiogenic stimuli in vitro

To investigate whether lymphatic vessel formation in vitro is modulated by known lymphangiogenic and anti-lymphangiogenic stimuli,

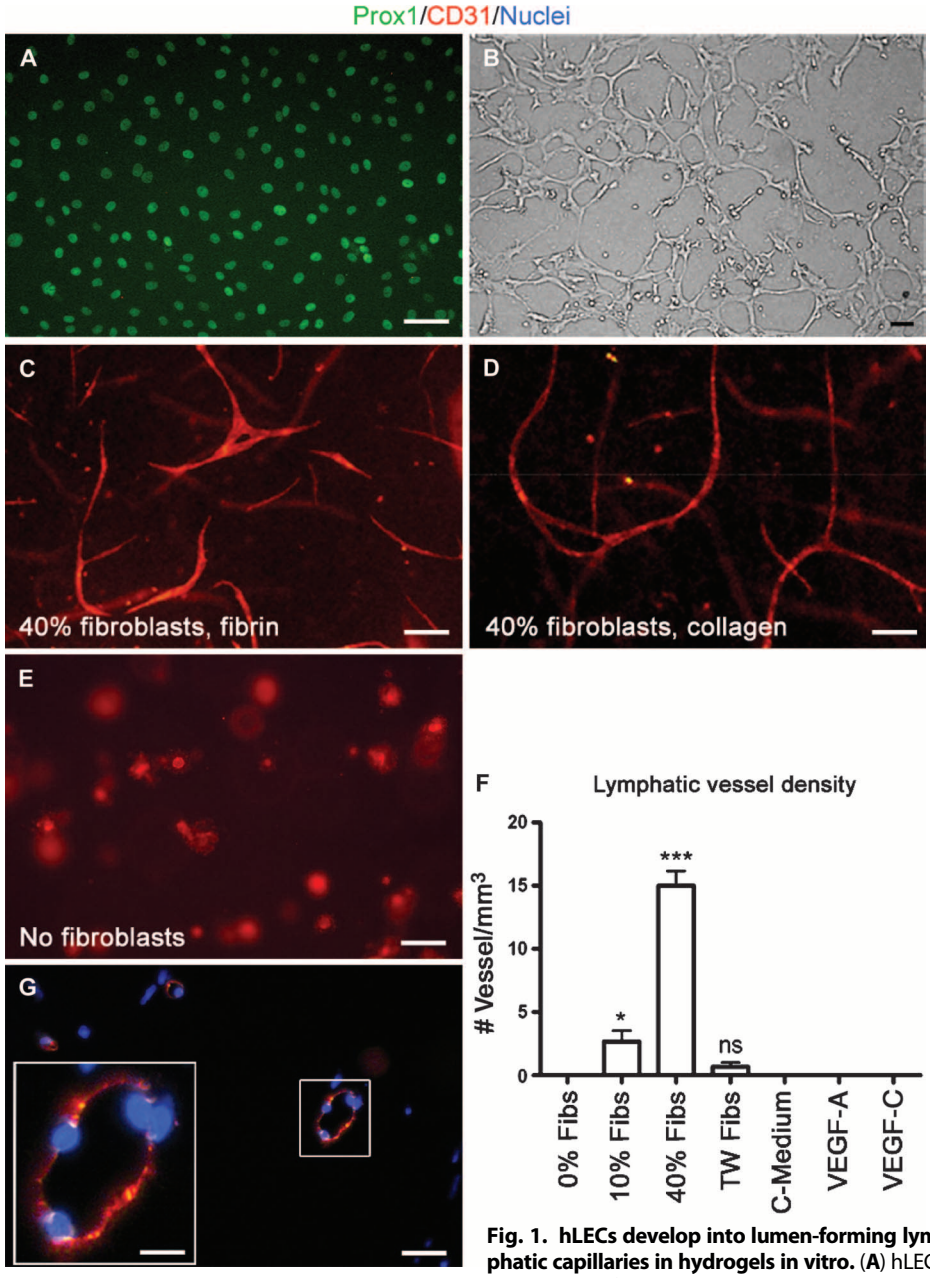

Fig. 1. hLECs develop into lumen-forming lymphatic capillaries in hydrogels in vitro. (**A**) hLECs express Prox1$^+$ (green). Scale bar, 50 μm. (**B**) hLECs assemble into cords in a 2D tube formation assay. Scale bar, 25 μm. (**C** to **E**) Whole-mount CD31 immunofluorescence analysis reveals that hLECs develop into capillaries when cocultured with human fibroblasts in either fibrin (C) or collagen (D) hydrogels, but not in the absence of human fibroblasts (E). Scale bars, 50 μm. (**F**) hLECs cultured in fibrin with 0 to 40% fibroblasts (Fibs), fibroblasts in a Transwell system (TW), human dermal fibroblasts–conditioned medium (C-Medium), VEGF-A, or VEGF-C. Data are means ± SEM (n = 6 hydrogels per group). *P < 0.05, ***P < 0.001, versus 0% fibroblasts using t test. ns, not significant. (**G**) Immunofluorescence analysis for CD31 (red) on paraffin sections shows lumen formation in lymphatic capillaries. Cell nuclei stained with 4′,6-diamidino-2-phenylindole (DAPI) (blue). Images are representative of n = 18 hydrogels. Scale bar, 10 μm (inset, 50 μm).

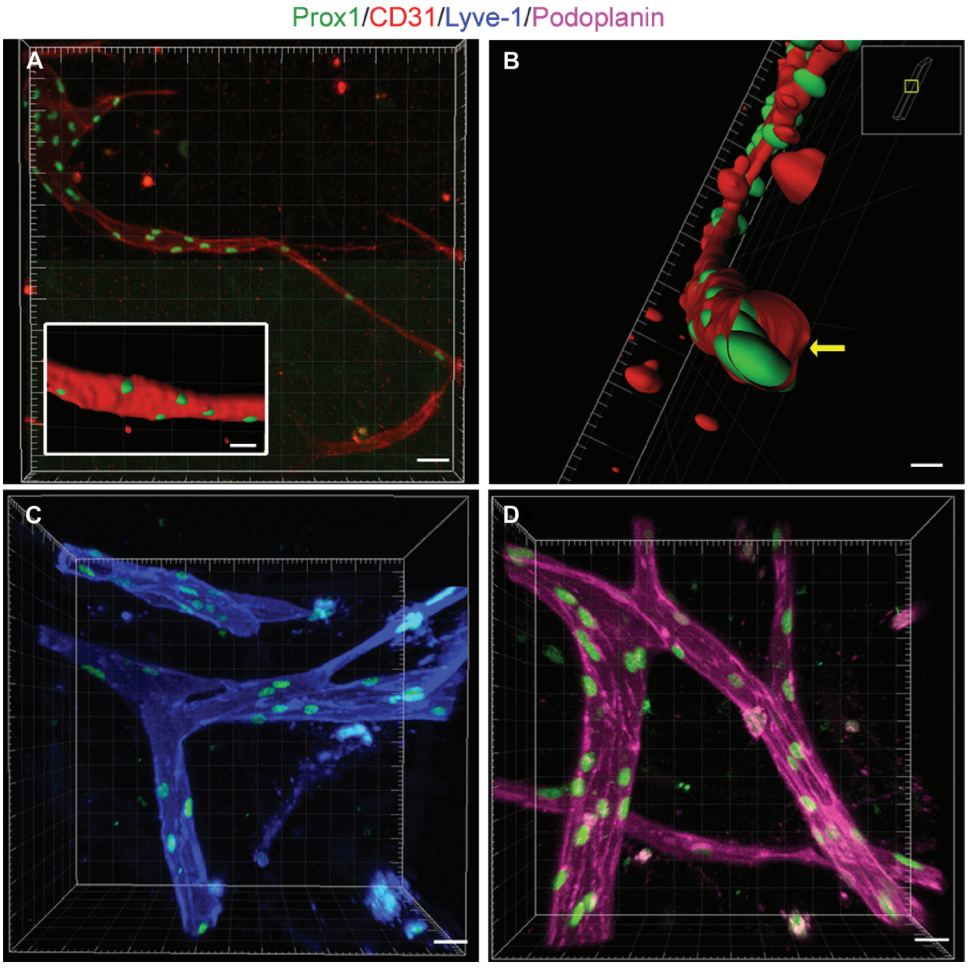

Fig. 2. In vitro bioengineered human lymphatic capillaries express lymphatic lineage-specific markers. (**A**) Whole-mount immunofluorescence analysis for CD31 (red) and Prox1 (green) confirms the lymphatic nature of the capillaries engineered in hLEC coculture with human dermal fibroblasts in fibrin hydrogels for 3 weeks in vitro. Scale bar, 50 μm (inset, 20 μm; digital surfacing caption). (**B**) The lymphatic capillary shown in (A) reveals the physiological distribution and size of Prox1$^+$ nuclei and the formation of a lumen (yellow arrow). Digital surfacing caption. Inset defines the spatial orientation of the snapshot. Scale bar, 3 μm. (**C** and **D**) Prox1$^+$ (green) lymphatic capillaries express both Lyve-1 (C, blue) and podoplanin (D, purple). Scale bars, 20 μm. Images are representative of n = 12 hydrogels. All images are confocal Z-stack captions; grids define the 3D space.

we investigated the effect of pro-lymphangiogenic VEGF-A and VEGF-C, as well as the effect of anti-lymphangiogenic transforming growth factor–β1 (TGF-β1) and the tyrosine kinase inhibitor SU5416 (*18*). Both VEGF-A and VEGF-C significantly promoted the formation of lymphatic capillaries in vitro compared to the factor-free control medium (Fig. 3, A to C and F). In contrast, exposure to SU5416 led to a significant inhibition of vessel formation (Fig. 3, D and F). Likewise, treatment with TGF-β1 significantly inhibited the formation of lymphatic microvessels (Fig. 3, E and F). Further analysis showed that hLECs tended to assemble into a slightly higher number of capillaries in type I collagen hydrogels compared to fibrin hydrogels in the presence or absence of VEGF-C (Fig. 3F). However, differences were not statistically significant.

Isolation of single-cell suspension from lymph-vascularized hydrogels

Studies on lymphatic vessel formation might necessitate specific molecular analysis at a cellular level to narrow down molecular pathways involved in lymphangiogenesis. Hence, we next investigated the possibility of retrieving single human cells from the lymph-vascularized hydrogels for further studies (Fig. 4A). Three weeks after in vitro culture, hLECs had assembled into CD31$^+$/Prox1$^+$ lymphatic capillaries as in Fig. 1D. At this stage, type I collagen hydrogels were digested using collagenase type II, and single cells were isolated and FACS-sorted into CD31$^+$/CD90$^-$ hLECs and CD31$^-$/CD90$^+$ fibroblasts (Fig. 4, B and C). After sorting, the individual populations of hydrogel-derived hLECs and fibroblasts were used to develop new lymph-vascularized hydrogels. The isolation/sorting procedure neither impaired the formation of the capillaries nor affected their lymphatic nature, as confirmed by whole-mount immunofluorescence staining for CD31 and Prox1 (Fig. 4, D and E).

Bioengineering a composite blood/lymphatic vascular plexus

On the basis of our ability to bioengineer blood capillaries and lymphatic capillaries in vitro, we focused on the generation of a complete dermal vascular plexus for skin grafting. This was achieved by coculturing HDMECs, isolated from human foreskin, in three-dimensional (3D) fibrin hydrogels. HDMECs consist of a mixture of both hLECs and human blood vascular endothelial cells (hBECs), as confirmed by a staining for Prox1 (Prox1$^+$ hLECs and Prox1$^-$ hBECs) (Fig. 5A). Coculture of HDMECs and human dermal fibroblasts in fibrin hydrogels for 3 weeks resulted in the formation of branching, lumenized capillaries (Fig. 5, B and C). Both Prox1$^+$/CD31$^+$ lymphatic capillaries and Prox1$^-$/CD31$^+$ blood capillaries were present in these hydrogels (Fig. 5D). In addition to Prox1, the two types of capillaries could also be discriminated using Lyve-1 (Fig. 5E). The two distinct types of microvessels were never found to anastomose in vitro; that is, they never formed hybrid blood-lymph capillaries. Similar to the hLEC cultures, HDMECs developed into lumen-forming capillaries in both fibrin (Fig. 5D) and collagen type I hydrogels (Fig. 5F).

To further investigate the functionality of the bioengineered lymphatic vessels, we determined whether the capillaries would react to interstitial pressure variations and resolve tissue fluid accumulation. Evans blue dye (20 to 80 μl) was injected into prevascularized hydrogels (Fig. 5G). After injection, CD31$^+$ and Lyve-1$^+$ lymphatic capillaries

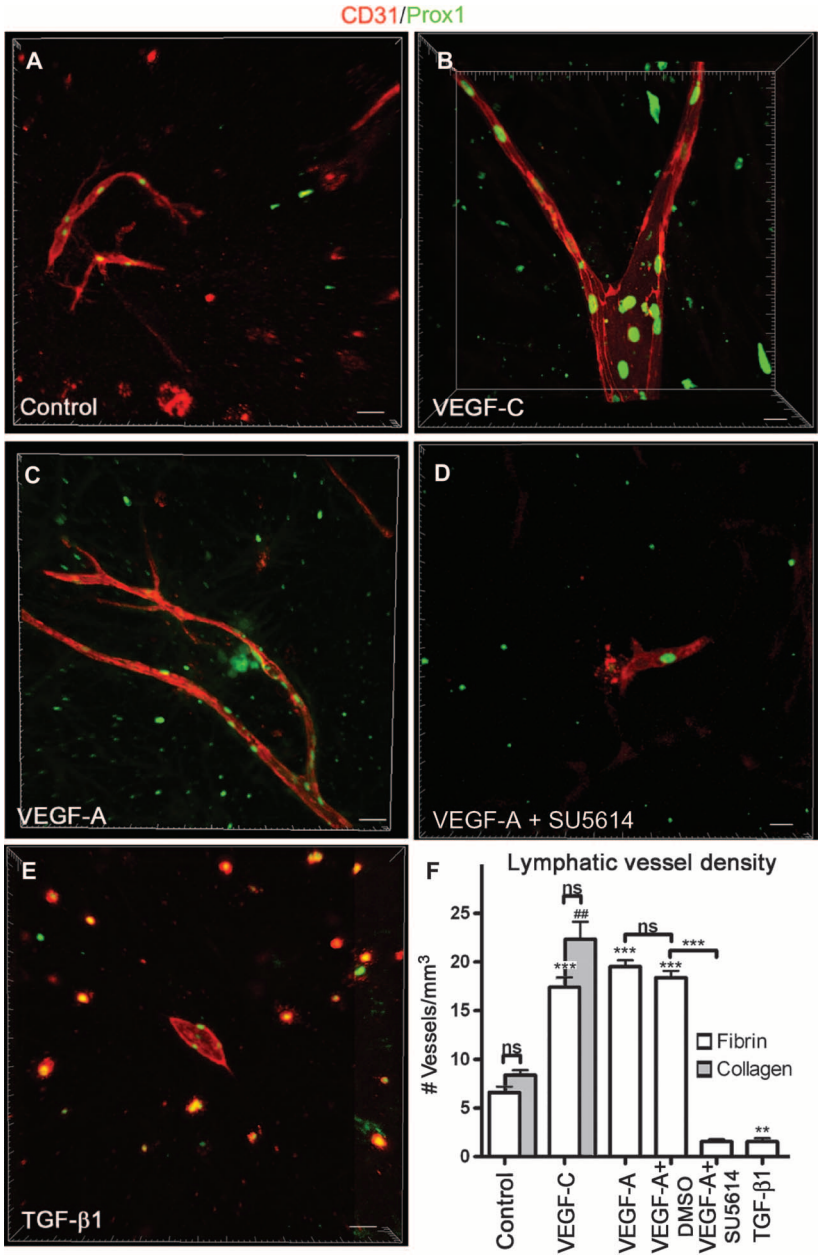

Fig. 3. In vitro bioengineered human lymphatic capillaries respond to lymphangiogenic and anti-lymphangiogenic stimuli. (**A**) Confocal microscopy of whole-mount immunofluorescence stainings for Prox1 (green) and CD31 (red) shows that hLECs, cultured in control medium, form capillaries in the fibrin hydrogels in vitro. Scale bar, 50 μm. (**B** and **C**) Exposure to VEGF-C (B) or VEGF-A (C) increases the density of branching lymphatic capillaries. (**D** and **E**) Exposure to SU5614 or TGF-β1 inhibits the formation of human lymphatic microvessels. Scale bars, 50 μm (C and E) and 20 μm (B and D). (**F**) The density of the lymphatic capillaries was quantified. Data are means ± SEM ($n = 6$ hydrogels per group). $^{**}P < 0.01$, $^{***}P < 0.001$ versus control fibrin hydrogels, unless otherwise indicated; $^{\#\#}P < 0.001$ versus control collagen hydrogels, *t* test. All *P* values were calculated against the respective control, unless otherwise specified. All images are displayed as Z-stack confocal captions; grid defines the 3D space.

were found to take up the dye from the extracellular space (Fig. 5H). Figure 5G shows that the area surrounding the lymphatic vessels was cleared from the dye after 20 minutes. These results show that the engineering of a dermal vascular plexus containing both blood and lymphatic capillaries is achievable and that the lymphatic capillaries exhibit their specific function, which is the uptake and removal of tissue liquid.

Human blood and lymphatic vascular plexus in bioengineered dermo-epidermal skin substitutes and in vivo grafting

Toward translation, we next monitored the transplantation of human dermo-epidermal skin grafts containing a composite vascular (blood and lymph) plexus onto rats. First, skin grafts were created in vitro using $CD31^+$ HDMECs, human $CD90^+$ fibroblasts, and human $keratin5^+$ ($K5^+$) keratinocytes in fibrin hydrogels. Figure 6A shows a confocal micrograph of a capillary (red) surrounded by fibroblasts (blue) in a fibrin hydrogel. Both cell types constituting the dermal compartment of the graft were arranged underneath several layers of keratinocytes (green), the epidermal compartment. These skin grafts were then transplanted onto wounded backs of immunoincompetent *nu/nu* rats using a Fusenig chamber to avoid competitive, lateral ingrowth/overgrowth of rat keratinocytes (Fig. 6B). The circular patch of the thin human epidermis was macroscopically visible. Two weeks after transplantation, the human skin substitute was surgically removed from the rat underlying tissue and analyzed for dermal structure and neovascularization. The vascularized neodermis supported stratification of the overlaying epidermis (Fig. 6C).

Immunofluorescence analysis after 2 weeks revealed the presence of both human blood and lymphatic microvessels in the neodermis (Fig. 6, D to H). Most of the bioengineered $Prox1^+/CD31^+$ lymphatic microvessels maintained their lumen in vivo (Fig. 6D, asterisks). Human microvessels expressing Lyve-1 and podoplanin were detected, indicating that human lymphatic capillaries remained intact 2 weeks after transplantation (Fig. 6E, arrow, and F to H). Blood microvessels that solely expressed CD31 were also detected (Fig. 6E, arrowhead). Notably, the two distinct types of microvessels were never found to anastomose. $Podoplanin^+$ lymphatic capillaries did not stain for laminin1,2 (Fig. 6F, arrow) but partially stained for collagen IV (Fig. 6G, arrows). Our analyses of mural cell (vascular smooth muscle cells and pericytes) coverage confirmed that the bioengineered human lymphatic capillaries were devoid of α-smooth muscle actin (αSMA)–expressing cells (Fig. 6H, arrows).

Further analysis of the capillary revealed that $podoplanin^+$ human lymphatic microvessels presented $fibrillin^+$ anchoring filaments (Fig. 6I, arrows). The presence of anchoring filaments strongly suggests that the capillaries could react to interstitial pressure variations and resolve tissue fluid accumulation in vivo. The presence of anchoring filaments and no or discontinuous basement membrane as well as the absence of mural cell coverage are major characteristics of lymphatic microvessels (*8*).

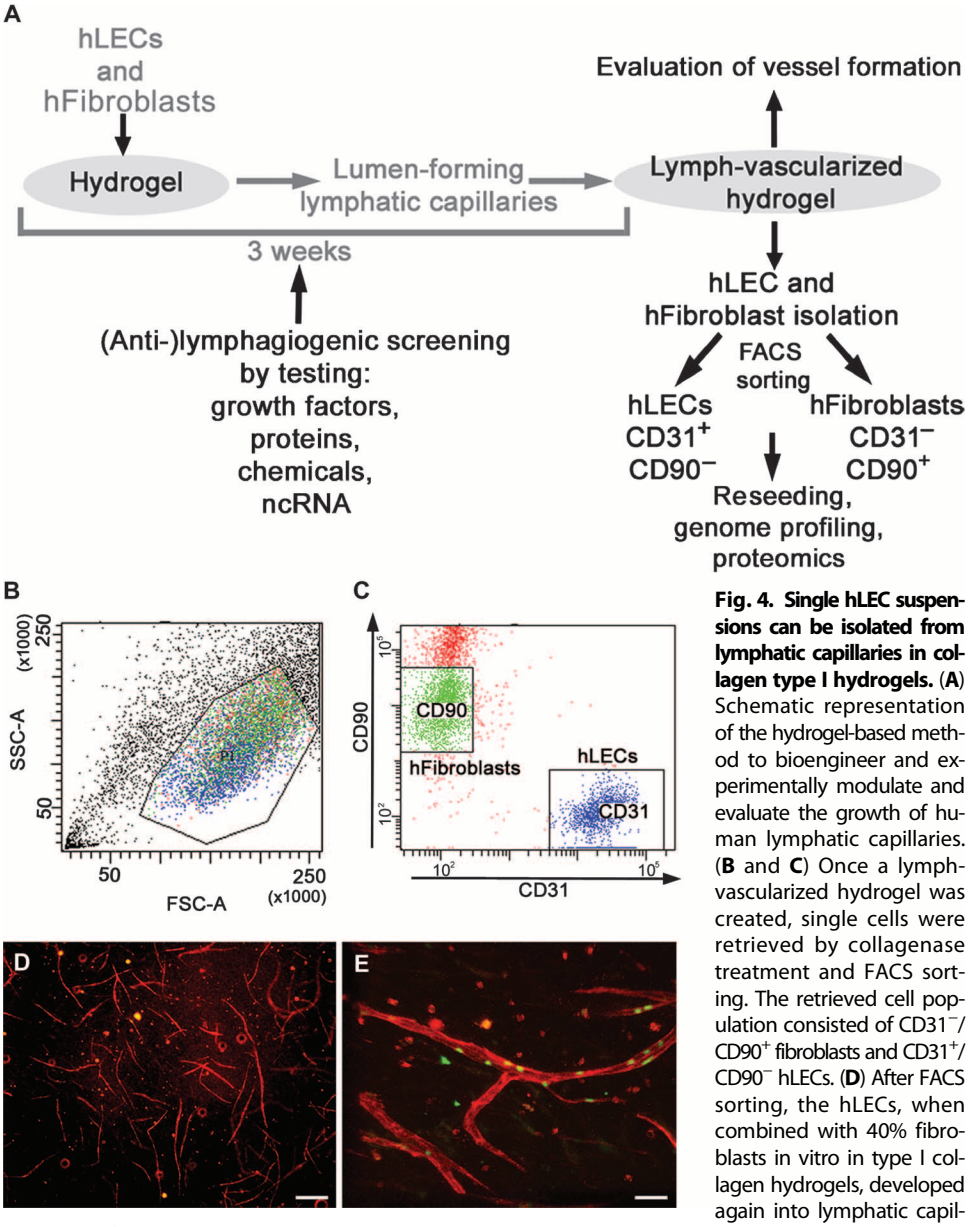

Fig. 4. Single hLEC suspensions can be isolated from lymphatic capillaries in collagen type I hydrogels. (**A**) Schematic representation of the hydrogel-based method to bioengineer and experimentally modulate and evaluate the growth of human lymphatic capillaries. (**B** and **C**) Once a lymph-vascularized hydrogel was created, single cells were retrieved by collagenase treatment and FACS sorting. The retrieved cell population consisted of CD31$^-$/CD90$^+$ fibroblasts and CD31$^+$/CD90$^-$ hLECs. (**D**) After FACS sorting, the hLECs, when combined with 40% fibroblasts in vitro in type I collagen hydrogels, developed again into lymphatic capillaries (CD31$^+$, red). Scale bar, 100 μm. (**E**) Capillaries in (D) expressed the lymphatic marker Prox1 (green). Scale bar, 40 μm. Images are representative of n = 12 hydrogels.

Anastomosis of bioengineered human lymphatic capillaries and in vivo functionality

Bioengineered blood vessels have been shown to connect to the host blood vasculature after in vivo grafting (*19*). We set out to investigate whether bioengineered lymphatic capillaries would also anastomose to the lymphatic vascular plexus of immunoincompetent recipient rats. The hydrogels were grafted to the wounded backs of *nu*/*nu* rats as in Fig. 6B. Immunofluorescence analyses of the expression of human- and rat-specific podoplanin showed that the human lymphatic capillaries, present in the bioengineered human dermis, connected to the host rat lymphatic vessels (3.5 + 2.6 SD anastomoses within a 0.5-mm stretch of bioengineered skin, total n = 8 animals) as early as 14 days after grafting (Fig. 7, A and B).

Hybrid anastomosis between human lymphatic capillaries and rat blood capillaries was never observed. We found two types of anastomoses among human and rat lymphatics: a direct connection type (Fig. 7A, arrow in inset) and a wrapping connection type (Fig. 7B, arrowheads in inset). The direct connection appeared to occur by linking of the blunt ends of a human and a rat lymphatic capillary. In the wrapping connection, the human and rat LECs wrapped around each other to form a hybrid vessel (Fig. 7B). Notably, rat lymphatics were found in close proximity to human lymphatic microvessels rather than randomly throughout the tissue (Fig. 7B).

To investigate whether the bioengineered lymphatic capillaries would be functional in vivo, we performed lymphatic drainage experiments by injecting small amounts (25 μl) of Evans blue into grafts 15 days after transplantation. When analyzing the grafts 30 minutes after injection, about five fold more Evans blue was retained in the hydrogels containing human fibroblasts only (Fig. 7C) compared with hydrogels containing human lymphatic and blood capillaries (Fig. 7, D and E), indicating lymphatic drainage function in the prevascularized grafts. These data suggest that the grafted human lymphatics were recognized by and anastomosed to the recipient's lymphatics and that the newly developed lymphatic plexus efficiently drained fluid in vivo.

DISCUSSION

Although structurally distinct, the blood and lymphatic vascular systems are functionally closely interconnected to ensure fluid and protein balance, cell nutrition, and immunologic functioning in tissues. The main function of the lymphatic system is the absorption of fluid and proteins that escaped from the blood circulation, hence, returning them back into the bloodstream. Impairment of lymphatic function leads to a number of diseases that are characterized by edema, seroma, lymphoceles, impaired immunity, and fibrosis (*8*). As the critical importance of the lymphatic system in the human body becomes more evident, tissue engineers are getting increasingly motivated to generate both blood and lymphatic vessels, side by side in bioengineered tissue and organ grafts (*20*).

Skin grafting is applied to treat defects caused by accident, such as burns, or in elective cases, such as scar revisions and removal of congenital nevi, or to treat chronic ulcers. Skin grafts may fail because of the development of infections, insufficient vascularization, hematoma,

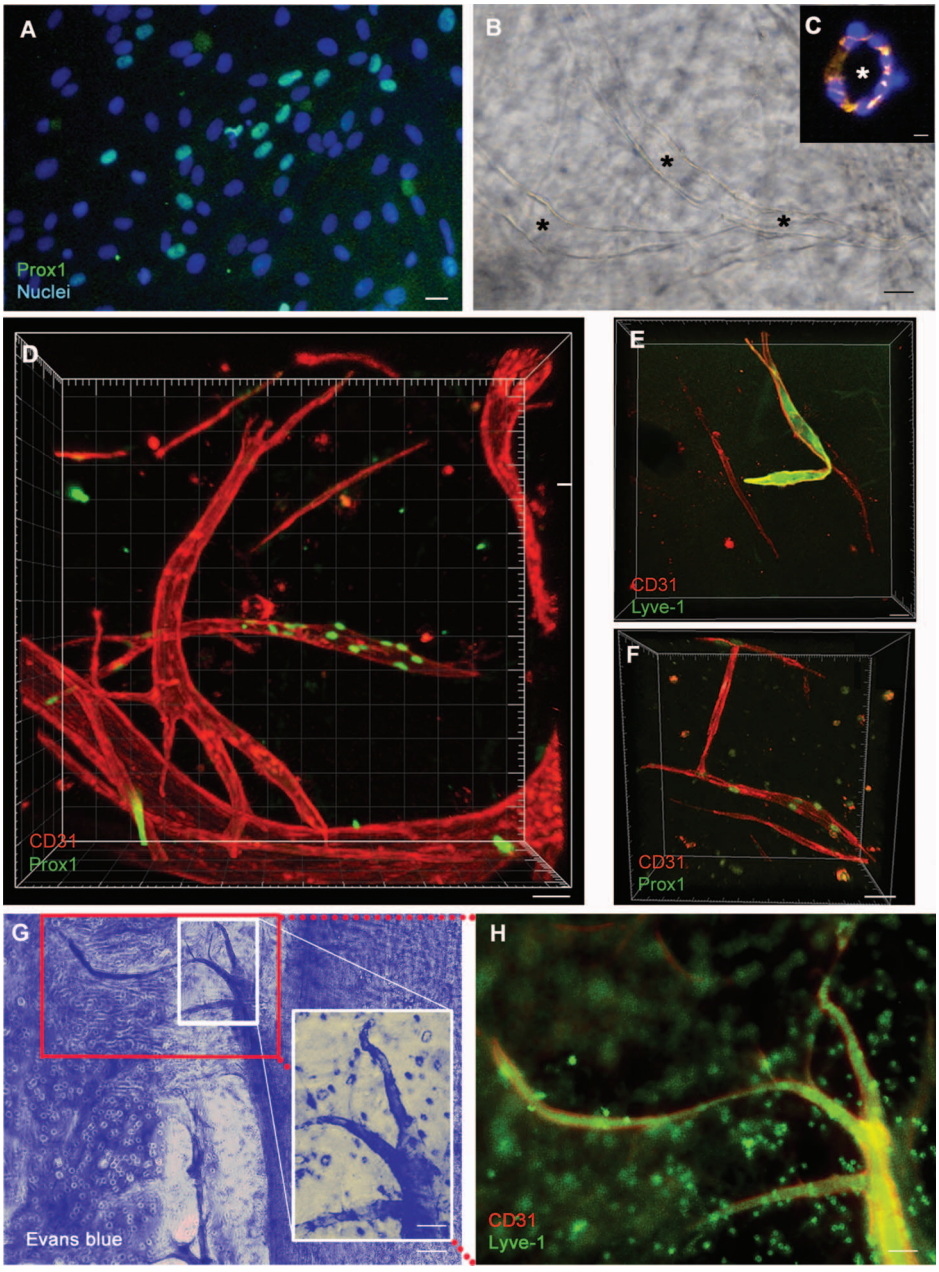

Fig. 5. HDMECs develop into blood capillaries as well as into functional lymphatic capillaries in fibrin hydrogels in vitro. (**A**) Immunofluorescence staining for the lymphatic marker Prox1 confirms that HDMECs isolated from human foreskin contain both Prox1$^+$ lymphatic (teal) and Prox1$^-$ blood vascular endothelial cells (blue only, for DAPI-stained nuclei). Scale bar, 25 μm. (**B** and **C**) Culture of HDMECs for 3 weeks in fibrin hydrogels resulted in the development of capillaries that presented a lumen (marked by asterisks). (B) Light microscopy of the hydrogel. (C) Immunofluorescence staining for CD31 [red cell nuclei (blue) of a paraffin-embedded hydrogel cross-section]. Scale bars, 10 μm (B and C). (**D**) Both Prox1$^+$/CD31$^+$ lymphatic and Prox1$^-$/CD31$^+$ blood capillaries were present in the 3D fibrin cultures. (**E**) Only the human lymphatic capillaries expressed the lymphatic marker Lyve-1 in the hydrogel. (**F**) HDMECs developed into both lymphatic and blood capillaries also in collagen type I hydrogels. Scale bars, 50 μm (D to F). (**G** and **H**) Evans blue dye injection into prevascularized fibrin hydrogels (n = 6) revealed that bioengineered human lymphatic capillaries take up fluid from the interstitial space (G). The same lymphatic vessel in (G) stains for CD31 and Lyve-1 (H). Scale bars, 50 μm [(G); inset, 20 μm] and 25 μm (H).

or seroma. Seromas occur by the accumulation of serous fluid underneath the graft because of the lack of sufficient drainage by the lymphatic system (*21*, *22*). Bioengineering a preformed network of lymphatic capillaries into dermo-epidermal skin grafts should help circumvent seroma formation by improving lymphatic drainage and accelerating the establishment of tissue fluid homeostasis.

In contrast to the large body of work done on the generation of blood vessels, only few studies have focused on engineering human lymphatic vasculature (*23*, *24*), including using a constant interstitial flow exerted by a bioreactor (*25*–*27*). The use of bioreactors is technically demanding, and, although it certainly represents a valid in vitro test system, no data are yet available on such engineered capillaries in vivo. A second pilot approach to tissue-engineered lymphatics indicated that hLECs could serve as seed cells to be combined with poly(glycolic acid) scaffolds (*28*). The developed tissue-engineered tubular structures showed very preliminary characteristics of a lymphangion (3-mm diameter); however, lymphatic capillaries, 10 to 60 μm in diameter (*29*), are required to constitute a functional, liquid-collecting, lymphatic plexus. The bioengineered lymphatic capillaries described herein showed exactly this range in diameter.

Our goal was to develop permanent, autologous dermo-epidermal skin grafts for clinical use. There are bioengineered grafts containing autologous keratinocytes and fibroblasts that are close to the clinical application, yet they are still not prevascularized (*30*–*36*). Here, we show that it is possible to even go beyond this approach by undertaking the bioengineering of prevascularized skin grafts that contain a blood and a lymphatic plexus in the dermal compartment. Successful bioengineering of lumen-forming lymphatic capillaries is owed to the coculture of fibroblasts with the endothelium because hLECs alone did not develop into lymphatic capillaries. Fibroblasts are known to rapidly migrate into wound sites to establish an extracellular matrix that supports dermal vascular repair. Thus, we speculate that, in our system, fibroblasts supported the formation of microvessels by creating a physiological environment by matrix remodeling and by production and deposition of nonsoluble factors; however,

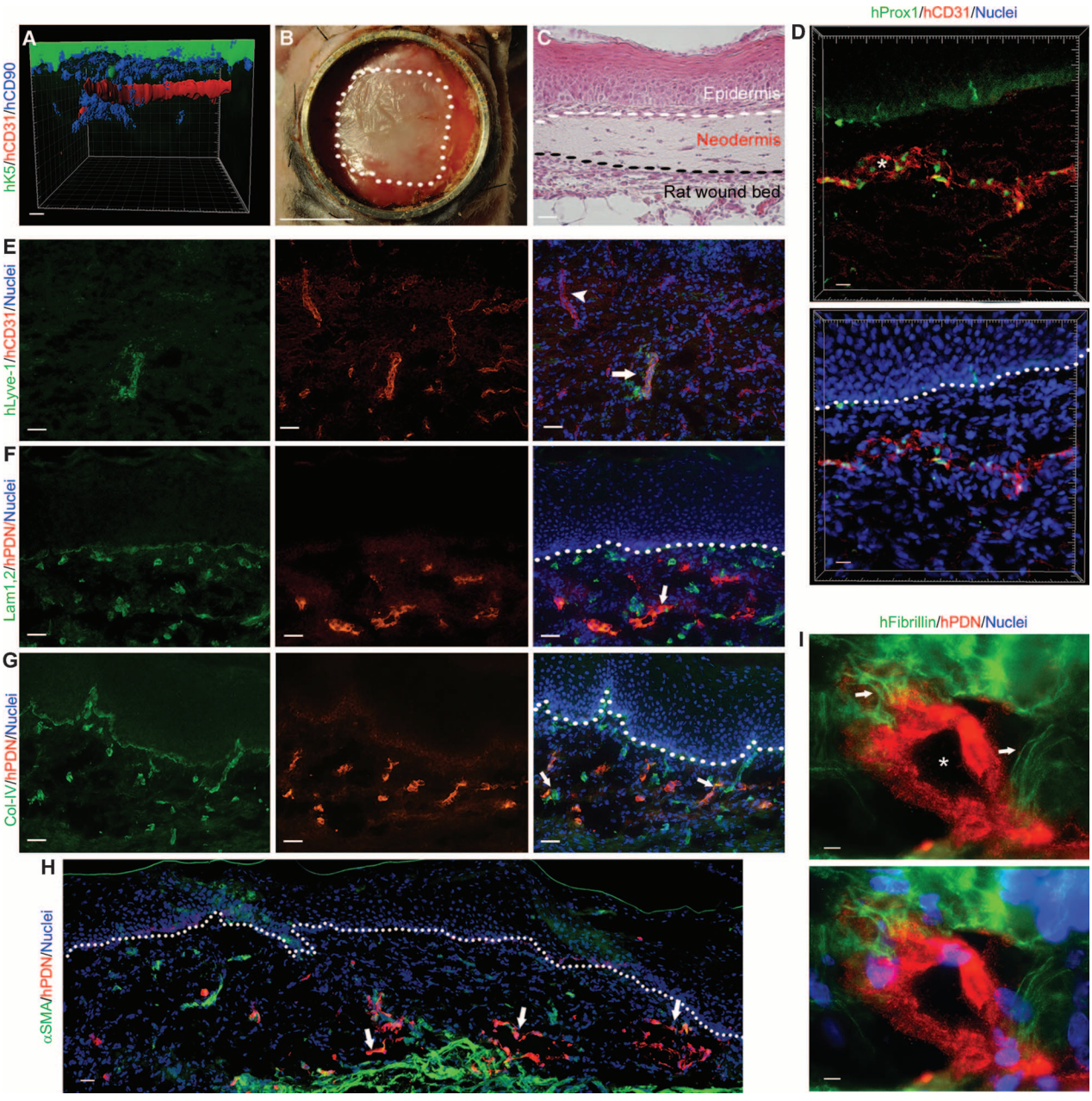

Fig. 6. Blood and lymphatic capillaries are stably maintained in bioengineered human dermo-epidermal skin grafts. Grafts were transplanted onto six rats. (**A**) Hydrogel-based prevascularized dermo-epidermal skin grafts were generated using CD31$^+$ HDMECs that form capillaries, CD90$^+$ human dermal fibroblasts, and human K5$^+$ keratinocytes (Z-stack confocal caption; digital surfacing; grid defines the 3D space). Scale bar, 50 μm. (**B**) The grafts were transplanted onto the backs of immunoincompetent *nu/nu* rats using a graft-protecting chamber. The dimensions of the bioengineered human skin are outlined in white. Scale bar, 1 cm. (**C**) After 2 weeks, hematoxylin and eosin staining revealed the presence of a stratified epidermis and a vascularized neodermis. Scale bar, 50 μm. (**D**) Immunofluorescence analysis of the transplants for human CD31 and Prox1 reveals the presence of a typical lymphatic capillary in the dermis. Asterisk denotes lumen. Cell nuclei were stained with DAPI, shown in bottom image (blue). Scale bars, 25 μm. (**E**) In contrast to the blood capillaries (expressing CD31 only, arrowhead), the lymphatic vessels expressed both human Lyve-1 and CD31 (costaining indicated by arrow). A vessel that expressed CD31 only is denoted by an arrowhead. (**F**) Expression of laminin (Lam1,2) was not detected on human podoplanin$^+$ (hPDN$^+$) lymphatic vessels (arrow). (**G**) The presence of an incomplete basement membrane on the hPDN$^+$ lymphatic capillaries was revealed by staining for collagen type IV (Col-IV, arrows). Scale bars, 100 μm (E to G). (**H**) αSMA-expressing mural cells were not found around the hPDN$^+$ lymphatic capillaries (arrows). Cell nuclei are stained with DAPI (blue). Dashed line indicates the dermo-epidermal junction. Scale bar, 50 μm. (**I**) Immunofluorescence analysis for human fibrillin shows the presence of anchoring filaments (arrows) on the hPDN$^+$ lymphatic capillaries. Asterisks indicate lumen. Scale bar, 10 μm.

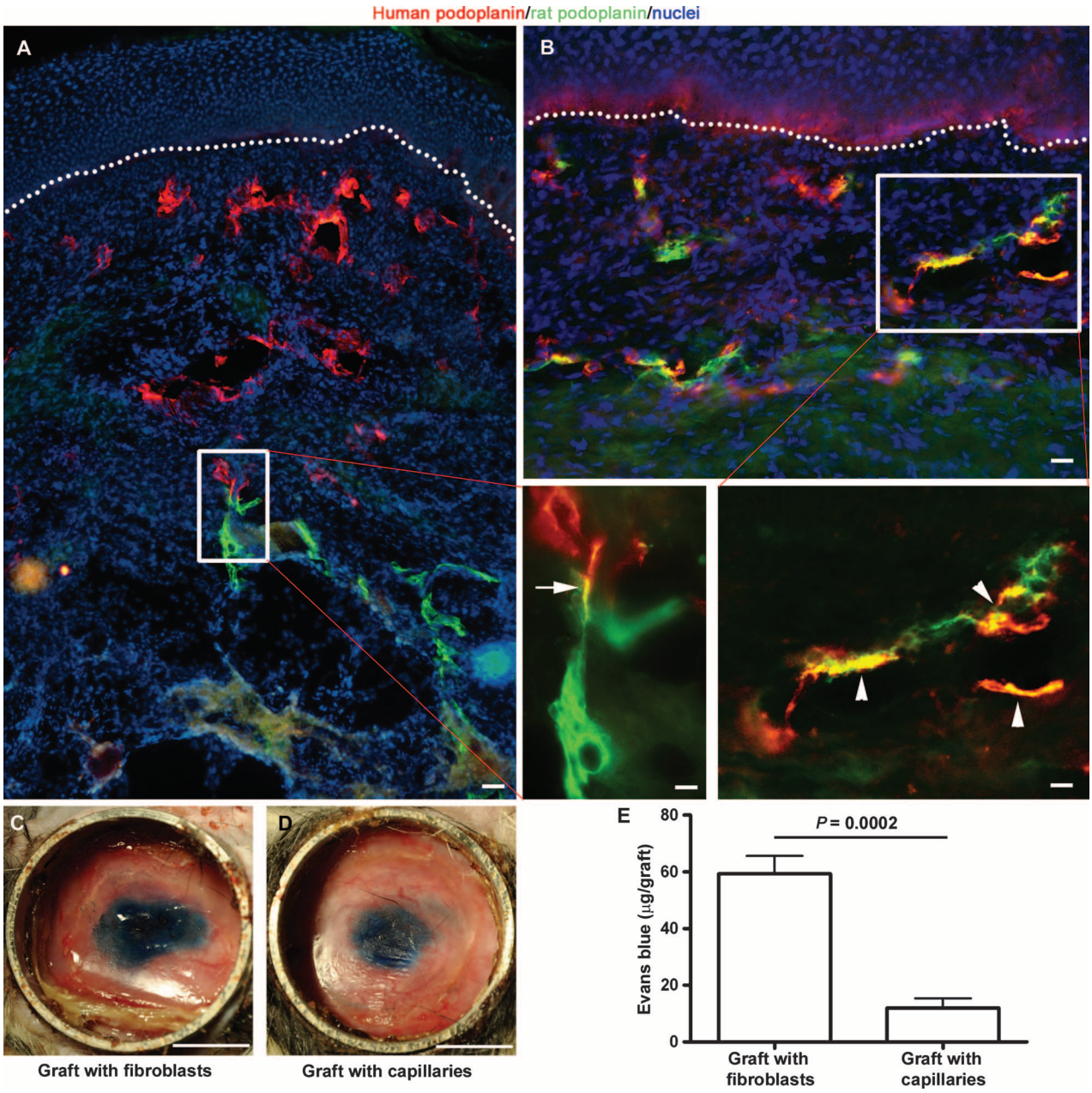

Fig. 7. Bioengineered human lymphatic capillaries anastomose to the recipient animal's lymphatic vasculature and drain fluid. Hydrogel-based, prevascularized dermo-epidermal skin grafts were transplanted onto the backs of immunoincompetent rats as in Fig. 6B. (**A** and **B**) As early as 14 days after transplantation, anastomosis occurred either as a "direct connection" [arrow in inset of (A)] or as a "wrapping connection" [arrowheads in inset of (B)]. Dashed lines indicate the dermo-epidermal junction. Nuclei are stained with DAPI (blue). Confocal images are representative of $n = 6$ animals. Scale bars, 100 μm (A) (magnified view, 35 μm) and 50 μm (B) (magnified view, 25 μm). (**C** to **E**) Fifteen days after transplantation, Evans blue dye was intradermally injected into grafts of four animals containing either only fibroblasts (C) or bioengineered human capillaries (D) and imaged and quantified (E) after 30 minutes. *P* value was determined by Student's *t* test. Scale bars, 1 cm (C and D).

this has not been demonstrated yet. This dermal environment modulation by fibroblasts might explain why, in our 3D hydrogel system, capillary formation occurred in both fibrin and collagen type I hydrogels.

The lymphatic nature of the generated capillaries was confirmed by the expression of lineage-specific markers, as well as by morphology and function. Expression of Prox1—the most specific marker for lymphatic endothelium (*15*, *16*)—Lyve-1, and podoplanin was detected in vitro and in vivo (*37*). The presence of fibrillin-containing anchoring filaments was detected on the human lymphatics, suggesting that the bioengineered capillaries might react to interstitial pressure variations in vivo. Finally, Evans blue dye uptake and drainage assay preliminarily confirmed that the bioengineered lymphatic capillaries were functional in vitro and in vivo, respectively. The lymphangiogenic factors VEGF-C and VEGF-A increased the lymphatic vessel density, whereas

the addition of the lymphangiogenesis inhibitors TGF-β1 and SU5614 resulted in decreased capillary formation. These modulatory induction/inhibition data, in addition to the possibility to retrieve the single cells from the hydrogels after vessel formation had occurred, qualify the 3D hydrogel system as a valuable in vitro model system and screening tool, well suited to identify signaling pathways, chemicals, and compounds involved in, or interfering with, human lymphatic vessel formation. In contrast to our system, most standard human lymphangiogenesis in vitro assays (*38*), such as the tube formation (*39*) or spheroid assays (*40*), are based on the evaluation of simple cord-like structures that only vaguely resemble the real morphology of bona fide lumen-forming human lymphatic capillaries.

When seeded in hydrogels, HDMECs, which consist of a mixture of hBECs and hLECs, spontaneously generated both a blood and a lymphatic vascular network, developing separately, yet adjacently in the same extracellular matrix. Although anastomoses between the two types of human vessels were never observed (*8*), the bioengineered human lymphatic capillaries were found to anastomose to the recipient rat's lymphatic plexus as early as 14 days after in vivo grafting. Human/rat lymphatic anastomosis occurred in either a direct connection or a wrapping connection manner. The "wrapping" anastomosis has been already described for blood vessels: The process includes matrix remodeling, pericyte removal, formation of a double-layered endothelium, and final maturation (*41*). Because the bioengineered lymphatic capillaries exhibited an incomplete basement membrane and no mural cell coverage, and because our immunofluorescence analyses revealed an overlapping of human/rat signals on microvessels, we suggest that the anastomosis of lymphatic microvessels by the wrapping mechanism could be brought about by the generation of a double-layered endothelium before maturation.

Clearly, the effects of the incorporation of a lymphatic plexus into a dermo-epidermal graft on its regeneration after transplantation will have to be further investigated. To satisfy regulatory and safety aspects of translation, leading to approval of this advanced technology for clinical use, these grafts will need to be preclinically tested on an immunocompetent animal model, such as the pig, to investigate on safety, toxicology, and efficacy.

With respect to skin, it is possible to generate complex human skin grafts, encompassing a dermal and an epidermal equivalent (*31*), a melanocyte compartment (*42*), and a plexus of blood and lymphatic capillaries (this study), whereas sweat glands, hair follicles, and neuronal innervation (*43*) have not yet been realized. Now, our study proposes a straightforward approach to engineer fully functional bona fide human lymphatic capillaries in hydrogel-based grafts, thus contributing to this broad spectrum of new possibilities in skin tissue engineering.

MATERIALS AND METHODS

Study design

The objective of this project was to engineer prevascularized dermo-epidermal human skin grafts containing human blood and lymphatic capillaries. First, hLECs were cocultured with human dermal fibroblasts within 3D hydrogels to investigate the capacity of LECs to develop into lumen-forming bona fide lymphatic capillaries. HDMECs—rather than LECs—were then used to engineer prevascularized dermo-epidermal skin substitutes. HDMECs were chosen because they are a mixture of dermal blood and LECs; hence, these cells have the potential to give rise to both types of capillaries. Prevascularized skin grafts were engineered using either collagen type I or fibrin hydrogels, demonstrating that, principally, both types of biomatrices can be successfully used. However, we mainly used fibrin hydrogels because those present higher mechanical stability than collagen hydrogels. Collagen hydrogels were used for the cell reisolation experiments because they are more easily digested than fibrin hydrogels. The morphology and functionality of the lymphatic microvessels were characterized and analyzed both in vitro and in vivo with immunofluorescence, FACS, histology, and Evans blue dye injection.

Statisticians at the University of Zurich were consulted regarding sample size. Briefly, sample size calculations were performed with a confidence level of 95% and a statistical power of 70 to 80%. In vitro, the experimental end point was chosen at 21 days, when most of the engineered capillaries had formed a lumen. In vivo, the experimental end point was 15 days, when epidermal stratification was completed and a basal lamina was deposited. Physical damage of the hydrogels or premature death of the animals resulted in the exclusion from the study. No outlier was encountered in the quantitative analyses. Animals or hydrogels were always assigned randomly to the experimental groups. The experiments were not blinded, with the exception of experiments evaluating the response of the engineered capillaries to anti-lymphangiogenic stimuli (Fig. 3). Three sample images were analyzed for each sample. All experiments were performed in triplicate.

Culture of hLECs

hLECs were purchased from ScienceCell. Cells were cultured in endothelial basal medium (Cambrex) supplemented with 20% fetal bovine serum (Gibco), L-glutamine (2 mM, Fluka), hydrocortisone (10 μg/ml, Fluka), and *N*-6,2′-odibutyryladenosine-3′,5′-cyclic monophosphate sodium salt (cAMP; 25 μg/ml, Fluka) for up to five passages. Cells were grown in a humidified atmosphere at 37°C and 5% CO_2. For the preparation of hydrogel matrices, cAMP was no longer added to the cultured medium, and endothelial cell supporting supplements (Cambrex) were added.

Isolation and culture of human dermal fibroblasts

Dermal fibroblasts were isolated from human foreskins obtained from the University Children's Hospital of Zurich after routine circumcisions and stored in Dulbecco's modified Eagle's medium supplemented with gentamicin, penicillin-streptomycin, and fungizone (Invitrogen). All patients (n = 6) (and/or their parents) gave their written consent for this study in accordance with the Ethics Commission of the Kanton Zurich (notification no. StV-12=06).

Human foreskin biopsies were digested for 15 to 18 hours at 4°C in dispase (12 U/ml) in Hanks' balanced salt solution containing gentamicin (5 mg/ml). Thereafter, the epidermis and the dermis were mechanically separated. After collagenase treatment of the dermis, a total of 4×10^6 dermal cells per 10-cm dish were grown in Dulbecco's modified Eagle's medium (DMEM) supplemented with 10% fetal calf serum, 4 mM L-alanyl-L-glutamine, 1 mM sodium pyruvate, and gentamicin (5 mg/ml). Collagenase was from Sigma-Aldrich, and all other compounds were from Invitrogen.

Isolation and culture of HDMECs and dermal fibroblasts

HDMECs and human dermal fibroblasts were co-isolated from foreskins (n = 8) obtained from the University Children's Hospital of Zurich after routine circumcisions (Ethics Commission notification no. StV-12=06). Foreskins were processed as described earlier (*7*). Isolated HDMECs

and fibroblasts were cocultured on 0.1% gelatin–coated dishes (Sigma-Aldrich) in endothelial cell growth medium-2 (EBM-2 MV with endothelial supplements; Lonza). Every day, fibroblasts were removed by mechanical scratching. FACS analysis for CD90 (Dianova) and CD31 (DakoCytomation) was used to calculate the number of fibroblasts and HDMEC (their ratio was 1:1 in all experiments). The cells were used at passage 1 in all experiments.

Generation of capillaries in hydrogels

Fibrin or collagen hydrogels were produced with a Transwell system (*7*) consisting of six-well culture inserts with membranes with 3-μm pores (BD Falcon). Briefly, for fibrin hydrogels, fibrinogen from bovine plasma (Sigma-Aldrich) was reconstituted in NaCl to a final concentration of 10 mg/ml, and then 11 μl of thrombin (Sigma-Aldrich, 100 U/ml) was added. For collagen hydrogels, membranes were covered with rat tail collagen type I hydrogels (3.2 to 3.4 mg/ml, BD Biosciences). The collagen matrix was prepared as described (*7*, *44*). To 1 ml of hydrogel solution, either 60,000 hLECs in combination with 40,000 human dermal fibroblasts or 100,000 human dermal cells (HDMECs/fibroblasts, 1:1) were added and transferred into an insert for six-well plates. After clotting at room temperature, the preparations were incubated at 37°C for 35 min in a humidified incubator containing 5% CO_2 to ensure polymerization. At the end of the incubation period, culture medium was added to the upper and lower chambers [endothelial cell growth medium-2 (EBM-2 MV with endothelial supplements; Lonza)], and hydrogels were incubated for up to 3 weeks. Medium was changed every second day.

The role of fibroblasts in lymphatic vessel formation

Fibrin hydrogels were produced as described above and cultured for 3 weeks in vitro. The hydrogels with 0 fibroblasts/100,000 LECs were cultured either in culture medium, in culture medium plus VEGF-A (40 ng/ml, Chemicon), in culture medium plus VEGF-C (100 ng/ml, R&D Systems), or in fibroblast-conditioned culture medium. The hydrogels with 10,000 fibroblasts/90,000 LECs or 40,000 fibroblasts/60,000 LECs were grown in culture medium. For the Transwell assay, 100,000 fibroblasts were seeded on the underside of the Transwell, whereas hydrogels with 100,000 LECs were cultured on top. The migration of a little number of fibroblasts was observed from the underside of the insert through the porous membrane intro the hydrogel. Culture medium was changed every day.

Validation of the lymphatic vessel formation in vitro assay

Hydrogels were prepared as described above. At day 0, VEGF-A (40 ng/ml) (Chemicon), VEGF-C (100 ng/ml) (R&D Systems), TGF-β1 (10 ng/ml) (R&D Systems), 10 μM dimethyl sulfoxide (Sigma), and 1,3-dihydro-3-[(3,5-dimethyl-1*H*-pyrrol-2-yl)methylene]-2*H*-indol-2-one (SU5416, Sigma) were added to the culture medium. The medium was changed every second day. After 3 weeks, gels were fixed in 4% paraformaldehyde (PFA) and processed for whole-mount immunostainings. Control culture medium was composed of endothelial basal medium (Cambrex) supplemented with 20% fetal bovine serum (Gibco), L-glutamine (2 mM, Fluka), and hydrocortisone (10 μg/ml, Fluka).

Isolation of single-cell suspensions from hydrogels containing lymphatic capillaries

At day 21, collagen type I hydrogels were incubated in a solution of collagenase type 2/DMEM (35 U/ml, Worthington Lakewood) for 1 hour at 37°C. After the incubation, single cells were collected by the use of cell strainers (0.40 μm, BD Pharmingen), centrifuged, counted, and prepared for FACS sorting (FACSAria III cell sorter, BD Biosciences). $CD31^+/CD90^-$ hLECs and $CD31^-/CD90^+$ human fibroblasts were sorted. The antibodies used were the following: mouse anti-human prelabeled CD31-phycoerythrin (DakoCytomation, 1:50) and monoclonal mouse anti-human prelabeled CD90–fluorescein isothiocyanate (Dianova, 1:10). Finally, the two cell populations were submerged again in gelifying collagen type I to test for the capability to develop into lymphatic capillaries.

Preparation of prevascularized skin grafts

After 2 weeks of culture, 1 million human keratinocytes, isolated as described (*31*), were seeded on top of the prevascularized fibrin hydrogels. One week thereafter, transplantation or whole-mount immunostaining was performed.

2D tube formation assay

Tube formation assays were performed as previously described (*45*). Briefly, a confluent hLEC monolayer was overlaid with collagen type I hydrogels (1 mg/ml; Cohesion). Tube-like structure formation was evaluated after 20 hours.

Evans blue fluid uptake in vitro assay

A solution of Evans blue (25 mg/ml) (Sigma-Aldrich) was prepared in phosphate-buffered saline (PBS). A total of 20 to 80 μl (focal injections of 20 μl) of this solution was laterally injected into a hydrogel with an insulin syringe (0.30 × 12 mm^2). After 20 min, hydrogels were analyzed under bright light. To remove excess dye, one washing step with PBS/0.3% Triton X overnight at room temperature and constant shaking were performed before the whole-mount immunofluorescence staining.

Grafting bioengineered skin grafts onto immunoincompetent *nu*/*nu* rats

Animal studies were performed with the approval of the Institutional Animal Care of the University of Zurich following the guidelines of the National Institutes of Health. Immunoincompetent female *nu*/*nu* rats (Elevage Janvier) (n = 12) were anesthetized by inhalation of 5% isoflurane (Baxter) and narcosis maintained by inhalation of 2.5% isoflurane via mask. Before the operation, buprenorphine (0.5 mg/kg) (Temgesic) for analgesia and retinol cream (Vitamin A "Blache"; Bausch & Lomb) for eye protection were applied. To prevent wound closure from the side and overgrowth of the human transplant by rat tissue, a special polypropylene ring (modified Fusenig chamber), 2.6 cm in diameter, was designed in our laboratory. The rings were sutured to full-thickness skin defects created on the back of the rats with nonabsorbable polyester sutures (Ethibond; Ethicon). Cultured prevascularized dermo-epidermal skin grafts were placed into the polypropylene rings and covered with a silicon foil (Silon-SES; Bio Med Sciences) and polyurethane sponges (Ligasano; Ligamed). Rats were sacrificed at 15 days after surgery. At sacrifice, dressings and sutures were removed, and multiple graft biopsies (n = 12) were collected for different analyses.

In vivo lymphatic drainage assessment with Evans blue dye

Fifteen days after transplantation on the rats, 25 μl of Evans blue dye (10 mg/ml in PBS, Sigma-Aldrich) was injected with a Hamilton syringe into hydrogel-based grafts. Thirty minutes later, pictures of the

grafts were taken. Subsequently, animals were sacrificed, and the Evans blue dye was extracted from the graft by incubation for 3 days in formamide (Fluka) at room temperature. The background-subtracted absorbance was measured on an Epoch microplate reader (Bio-Tek) by measuring the wavelength at 620 and 740 nm. The concentration of dye in the extracts was calculated with a standard curve of Evans blue in formamide.

Immunofluorescence stainings and quantifications

Hydrogel matrices were collected and fixed in 4% PFA for 6 hours at room temperature and processed for either whole-mount immunostainings or paraffin/cryo embedding and cutting.

For whole-mount immunostainings, samples were blocked with 10% bovine serum albumin (Sigma-Aldrich) and 0.3% Triton X (Sigma-Aldrich) in PBS. Primary and secondary antibodies were applied overnight at room temperature. Washing steps were performed with PBS and 0.3% Triton X. For paraffin preparations, samples were dehydrated and mounted in paraffin wax. For cryosections, samples were frozen in OCT compound (Tissue-Tek). Cross-sections (10 or 40 μm) were cut and mounted on glass slides. For all immunofluorescence procedures, the following primary antibodies were used: rabbit anti-human Prox1 (Reliatech; 1:300), monoclonal mouse anti-human CD31 (DakoCytomation; 1:50), monoclonal mouse anti-human CD90 (Dianova; 1:10), rabbit anti-human Lyve-1 (Abcam; 1:100), mouse anti-human podoplanin (Santa Cruz Biotechnology, 1:50), mouse anti-human αSMA (DakoCytomation), mouse anti-rat podoplanin (Reliatech), mouse anti-human collagen IV (Abcam), mouse anti-human fibrillin (Millipore), and mouse anti-human laminin 1+2 (Abcam). Corresponding secondary antibodies were labeled with Alexa Fluor 488 or 594 (Molecular Probes). Cell nuclei were counterstained with Hoechst bisbenzimide (Sigma-Aldrich). Stained specimens were examined with a Nikon Eclipse TE-2000-U confocal microscope. Adobe Photoshop CS3 (Adobe Systems) was used for image overlay. The Imaris software (Bitplane AG) was used to create 3D pictures (Z-stack) and digital surface images of confocal data. Computer-assisted morphometric vessel analyses were performed with Adobe Photoshop CS3. The average vessel area and vessel number per group were calculated, and statistical analysis was performed with GraphPad Prism (GraphPad Software Inc.).

Statistical analysis

The statistical analysis was carried out with the software GraphPad Prism. Student's *t* test, paired, two-tailed, with 95% confidence interval, without adjustments to α levels, was used for all comparisons. $P < 0.05$ was considered significant. Data are shown as means ± SEM.

REFERENCES AND NOTES

1. A. Atala, F. K. Kasper, A. G. Mikos, Engineering complex tissues. *Sci. Transl. Med.* **4**, 160rv12 (2012).
2. S. Böttcher-Haberzeth, T. Biedermann, E. Reichmann, Tissue engineering of skin. *Burns* **36**, 450–460 (2010).
3. H. Bae, A. S. Puranik, R. Gauvin, F. Edalat, B. Carrillo-Conde, N. A. Peppas, A. Khademhosseini, Building vascular networks. *Sci. Transl. Med.* **4**, 160ps23 (2012).
4. A. F. Black, F. Berthod, N. L'Heureux, L. Germain, F. A. Auger, In vitro reconstruction of a human capillary-like network in a tissue-engineered skin equivalent. *FASEB J.* **12**, 1331–1340 (1998).
5. L. Gibot, T. Galbraith, J. Huot, F. A. Auger, A preexisting microvascular network benefits in vivo revascularization of a microvascularized tissue-engineered skin substitute. *Tissue Eng. Part A* **16**, 3199–3206 (2010).
6. D. M. Supp, K. Wilson-Landy, S. T. Boyce, Human dermal microvascular endothelial cells form vascular analogs in cultured skin substitutes after grafting to athymic mice. *FASEB J.* **16**, 797–804 (2002).
7. I. Montaño, C. Schiestl, J. Schneider, L. Pontiggia, J. Luginbühl, T. Biedermann, S. Böttcher-Haberzeth, E. Braziulis, M. Meuli, E. Reichmann, Formation of human capillaries in vitro: The engineering of prevascularized matrices. *Tissue Eng. Part A* **16**, 269–282 (2010).
8. M. Skobe, M. Detmar, Structure, function, and molecular control of the skin lymphatic system. *J. Investig. Dermatol. Symp. Proc.* **5**, 14–19 (2000).
9. R. Gerli, R. Solito, E. Weber, M. Aglianó, Specific adhesion molecules bind anchoring filaments and endothelial cells in human skin initial lymphatics. *Lymphology* **33**, 148–157 (2000).
10. A. Henno, S. Blacher, C. Lambert, A. Colige, L. Seidel, A. Noël, C. Lapière, M. de la Brassinne, B. V. Nusgens, Altered expression of angiogenesis and lymphangiogenesis markers in the uninvolved skin of plaque-type psoriasis. *Br. J. Dermatol.* **160**, 581–590 (2009).
11. R. Kunstfeld, S. Hirakawa, Y. K. Hong, V. Schacht, B. Lange-Asschenfeldt, P. Velasco, C. Lin, E. Fiebiger, X. Wei, Y. Wu, D. Hicklin, P. Bohlen, M. Detmar, Induction of cutaneous delayed-type hypersensitivity reactions in VEGF-A transgenic mice results in chronic skin inflammation associated with persistent lymphatic hyperplasia. *Blood* **104**, 1048–1057 (2004).
12. F. Pedica, C. Ligorio, P. Tonelli, S. Bartolini, P. Baccarini, Lymphangiogenesis in Crohn's disease: An immunohistochemical study using monoclonal antibody D2-40. *Virchows Arch.* **452**, 57–63 (2008).
13. A. Saaristo, T. Tammela, A. Farkkilä, M. Kärkkäinen, E. Suominen, S. Yla-Herttuala, K. Alitalo, Vascular endothelial growth factor-C accelerates diabetic wound healing. *Am. J. Pathol.* **169**, 1080–1087 (2006).
14. E. Kriehuber, S. Breiteneder-Geleff, M. Groeger, A. Soleiman, S. F. Schoppmann, G. Stingl, D. Kerjaschki, D. Maurer, Isolation and characterization of dermal lymphatic and blood endothelial cells reveal stable and functionally specialized cell lineages. *J. Exp. Med.* **194**, 797–808 (2001).
15. Y. K. Hong, N. Harvey, Y. H. Noh, V. Schacht, S. Hirakawa, M. Detmar, G. Oliver, Prox1 is a master control gene in the program specifying lymphatic endothelial cell fate. *Dev. Dyn.* **225**, 351–357 (2002).
16. J. T. Wigle, N. Harvey, M. Detmar, I. Lagutina, G. Grosveld, M. D. Gunn, D. G. Jackson, G. Oliver, An essential role for *Prox1* in the induction of the lymphatic endothelial cell phenotype. *EMBO J.* **21**, 1505–1513 (2002).
17. K. Hida, Y. Hida, D. N. Amin, A. F. Flint, D. Panigrahy, C. C. Morton, M. Klagsbrun, Tumor-associated endothelial cells with cytogenetic abnormalities. *Cancer Res.* **64**, 8249–8255 (2004).
18. T. A. Fong, L. K. Shawver, L. Sun, C. Tang, H. App, T. J. Powell, Y. H. Kim, R. Schreck, X. Wang, W. Risau, A. Ullrich, K. P. Hirth, G. McMahon, SU5416 is a potent and selective inhibitor of the vascular endothelial growth factor receptor (Flk-1/KDR) that inhibits tyrosine kinase catalysis, tumor vascularization, and growth of multiple tumor types. *Cancer Res.* **59**, 99–106 (1999).
19. S. Levenberg, J. Rouwkema, M. Macdonald, E. S. Garfein, D. S. Kohane, D. C. Darland, R. Marini, C. A. van Blitterswijk, R. C. Mulligan, P. A. D'Amore, R. Langer, Engineering vascularized skeletal muscle tissue. *Nat. Biotechnol.* **23**, 879–884 (2005).
20. N. C. Rivron, J. J. Liu, J. Rouwkema, J. de Boer, C. A. van Blitterswijk, Engineering vascularised tissues in vitro. *Eur. Cell. Mater.* **15**, 27–40 (2008).
21. S. Gupta, Optimal use of negative pressure wound therapy for skin grafts. *Int. Wound J.* **9** (Suppl. 1), 40–47 (2012).
22. L. Jewell, R. Guerrero, A. R. Quesada, L. S. Chan, W. L. Garner, Rate of healing in skin-grafted burn wounds. *Plast. Reconstr. Surg.* **120**, 451–456 (2007).
23. T. Hitchcock, L. Niklason, Lymphatic tissue engineering: Progress and prospects. *Ann. N. Y. Acad. Sci.* **1131**, 44–49 (2008).
24. L. E. Niklason, J. Koh, A. Solan, Tissue engineering of the lymphatic system. *Ann. N. Y. Acad. Sci.* **979**, 27–34; discussion 35–38 (2002).
25. C. L. Helm, A. Zisch, M. A. Swartz, Engineered blood and lymphatic capillaries in 3-D VEGF-fibrin-collagen matrices with interstitial flow. *Biotechnol. Bioeng.* **96**, 167–176 (2007).
26. C. P. Ng, C. L. Helm, M. A. Swartz, Interstitial flow differentially stimulates blood and lymphatic endothelial cell morphogenesis in vitro. *Microvasc. Res.* **68**, 258–264 (2004).
27. C. L. Helm, M. E. Fleury, A. H. Zisch, F. Boschetti, M. A. Swartz, Synergy between interstitial flow and VEGF directs capillary morphogenesis in vitro through a gradient amplification mechanism. *Proc. Natl. Acad. Sci. U.S.A.* **102**, 15779–15784 (2005).
28. Tt. Dai, Zh. Jiang, Sl. Li, Gd. Zhou, J. D. Kretlow, Wg. Cao, W. Liu, Yl. Cao, Reconstruction of lymph vessel by lymphatic endothelial cells combined with polyglycolic acid scaffolds: A pilot study. *J. Biotechnol.* **150**, 182–189 (2010).
29. K. N. Margaris, R. A. Black, Modelling the lymphatic system: Challenges and opportunities. *J. R. Soc. Interface* **9**, 601–612 (2012).
30. E. Braziulis, T. Biedermann, F. Hartmann-Fritsch, C. Schiestl, L. Pontiggia, S. Böttcher-Haberzeth, E. Reichmann, M. Meuli, Skingineering I: Engineering porcine dermo-epidermal skin analogues for autologous transplantation in a large animal model. *Pediatr. Surg. Int.* **27**, 241–247 (2011).

31. E. Braziulis, M. Diezi, T. Biedermann, L. Pontiggia, M. Schmucki, F. Hartmann-Fritsch, J. Luginbühl, C. Schiestl, M. Meuli, E. Reichmann, Modified plastic compression of collagen hydrogels provides an ideal matrix for clinically applicable skin substitutes. *Tissue Eng. Part C Methods* **18**, 464–474 (2012).
32. E. Reichmann, EuroSkinGraft: Novel generation of skin substitutes to clinically treat a broad spectrum of severe skin defects, FP7/2007-2013 grant agreement no. 279024; http://www.euroskingraft.eu.
33. C. Schiestl, T. Biedermann, E. Braziulis, F. Hartmann-Fritsch, S. Böttcher-Haberzeth, M. Arras, N. Cesarovic, F. Nicolls, C. Linti, E. Reichmann, M. Meuli, Skingineering II: Transplantation of large-scale laboratory-grown skin analogues in a new pig model. *Pediatr. Surg. Int.* **27**, 249–254 (2010).
34. R. V. Shevchenko, S. L. James, S. E. James, A review of tissue-engineered skin bioconstructs available for skin reconstruction. *J. R. Soc. Interface* **7**, 229–258 (2010).
35. Regenicin, Permaderm; http://www.regenicin.com/about/about-permaderm.html.
36. A. Feuerstein, FDA did not approve Regenicin skin graft; http://www.thestreet.com/story/11579041/1/fda-did-not-approve-regenicin-skin-graft.html.
37. A. Alajati, A. M. Laib, H. Weber, A. M. Boos, A. Bartol, K. Ikenberg, T. Korff, H. Zentgraf, C. Obodozie, R. Graeser, S. Christian, G. Finkenzeller, G. B. Stark, M. Héroult, H. G. Augustin, Spheroid-based engineering of a human vasculature in mice. *Nat. Methods* **5**, 439–445 (2008).
38. F. Bruyère, A. Noël, Lymphangiogenesis: In vitro and in vivo models. *FASEB J.* **24**, 8–21 (2010).
39. V. Schacht, M. I. Ramirez, Y. K. Hong, S. Hirakawa, D. Feng, N. Harvey, M. Williams, A. M. Dvorak, H. F. Dvorak, G. Oliver, M. Detmar, T1α/podoplanin deficiency disrupts normal lymphatic vasculature formation and causes lymphedema. *EMBO J.* **22**, 3546–3556 (2003).
40. Y. Xu, L. Yuan, J. Mak, L. Pardanaud, M. Caunt, I. Kasman, B. Larrivée, R. Del Toro, S. Suchting, A. Medvinsky, J. Silva, J. Yang, J. L. Thomas, A. W. Koch, K. Alitalo, A. Eichmann, A. Bagri, Neuropilin-2 mediates VEGF-C–induced lymphatic sprouting together with VEGFR3. *J. Cell Biol.* **188**, 115–130 (2010).
41. G. Cheng, S. Liao, H. Kit Wong, D. A. Lacorre, E. di Tomaso, P. Au, D. Fukumura, R. K. Jain, L. L. Munn, Engineered blood vessel networks connect to host vasculature via wrapping-and-tapping anastomosis. *Blood* **118**, 4740–4749 (2011).
42. S. Böttcher-Haberzeth, A. S. Klar, T. Biedermann, C. Schiestl, C. Meuli-Simmen, E. Reichmann, M. Meuli, "Trooping the color": Restoring the original donor skin color by addition of melanocytes to bioengineered skin analogs. *Pediatr. Surg. Int.* **29**, 239–247 (2013).
43. T. Biedermann, S. Böttcher-Haberzeth, A. S. Klar, L. Pontiggia, C. Schiestl, C. Meuli-Simmen, E. Reichmann, M. Meuli, Rebuild, restore, reinnervate: Do human tissue engineered dermo-epidermal skin analogs attract host nerve fibers for innervation? *Pediatr. Surg. Int.* **29**, 71–78 (2013).
44. D. E. Costea, L. L. Loro, E. A. Dimba, O. K. Vintermyr, A. C. Johannessen, Crucial effects of fibroblasts and keratinocyte growth factor on morphogenesis of reconstituted human oral epithelium. *J. Invest. Dermatol.* **121**, 1479–1486 (2003).
45. K. Kajiya, S. Hirakawa, B. Ma, I. Drinnenberg, M. Detmar, Hepatocyte growth factor promotes lymphatic vessel formation and function. *EMBO J.* **24**, 2885–2895 (2005).

Acknowledgments: We are grateful to E. Manuel for helping with the human skin sample collection. **Funding:** This work was supported by two grants from the European Union (EuroSTEC: LSHB-CT-2006-037409 and EuroSkinGraft: FP7/2007-2013 grant agreement no. 279024) and the Clinical Research Priority Programs of the Faculty of Medicine of the University of Zurich. We are particularly grateful to the Foundation Gaydoul and the sponsors of "DonaTissue" (T. Meier and R. Zingg) for their financial support and their interest in our work. **Author contributions:** D.M. designed the study, performed the experiments, analyzed the data, and wrote and reviewed the manuscript. J.L. designed the study, performed the experiments, analyzed the data, and reviewed the manuscript. S.S. performed the experiments. M.M. discussed the data and reviewed the manuscript. E.R. designed the study, discussed the data, and wrote and reviewed the manuscript. **Competing interests:** The authors declare that they have no competing interests. **Data and materials availability:** A materials transfer agreement is required for transfer of materials.

Submitted 26 June 2013
Accepted 8 January 2014
Published 29 January 2014
10.1126/scitranslmed.3006894

Citation: D. Marino, J. Luginbühl, S. Scola, M. Meuli, E. Reichmann, Bioengineering dermo-epidermal skin grafts with blood and lymphatic capillaries. *Sci. Transl. Med.* **6**, 221ra14 (2014).